Lawrence Berkeley National Laboratory
LBL Publications

Title

Simulation of Transport Equations for Unstable Systems: Comparison Between Lattice and Test-Particle Methods

Permalink

https://escholarship.org/uc/item/2z5204zq

Authors

Burgio, G.S.
Chomaz, Ph.
Colonna, M.
et al.

Publication Date

1994-09-30

eScholarship.org Powered by the California Digital Library
University of California

LBL-35998
UC-413
Preprint

Lawrence Berkeley Laboratory
UNIVERSITY OF CALIFORNIA

Submitted to Nuclear Physics A

Simulation of Transport Equations for Unstable Systems: Comparison between lattice and test-particle methods

G.F. Burgio, Ph. Chomaz, M. Colonna, and J. Randrup

September 1994

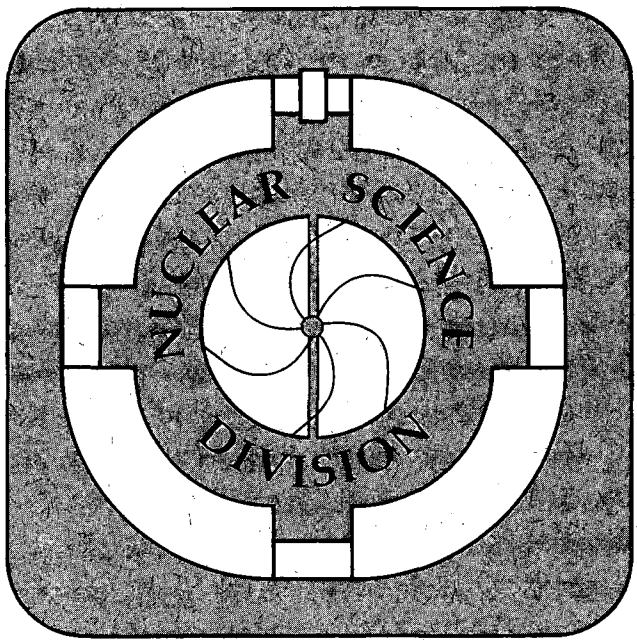

REFERENCE COPY
Does Not
Circulate
LBL-35998
Copy 1
Bldg. 50 Library.

Prepared for the U.S. Department of Energy under Contract Number DE-AC03-76SF00098

DISCLAIMER

This document was prepared as an account of work sponsored by the United States Government. While this document is believed to contain correct information, neither the United States Government nor any agency thereof, nor the Regents of the University of California, nor any of their employees, makes any warranty, express or implied, or assumes any legal responsibility for the accuracy, completeness, or usefulness of any information, apparatus, product, or process disclosed, or represents that its use would not infringe privately owned rights. Reference herein to any specific commercial product, process, or service by its trade name, trademark, manufacturer, or otherwise, does not necessarily constitute or imply its endorsement, recommendation, or favoring by the United States Government or any agency thereof, or the Regents of the University of California. The views and opinions of authors expressed herein do not necessarily state or reflect those of the United States Government or any agency thereof or the Regents of the University of California.

Nuclear Physics LBL-35998

Simulation of Transport Equations for Unstable Systems: Comparison between lattice and test-particle methods *

G.F. Burgio[1], *Ph. Chomaz*[2], *M. Colonna*[2,3], *and J. Randrup*[4]

[1)] Dipartimento di Fisica, Universita' di Catania and INFN Sezione di Catania, 57 Corso Italia, I-95129 Catania, Italy

[2)] GANIL, B.P. 5027, F-14021 Caen Cedex, France

[3)] Laboratorio Nazionale del Sud, Viale Andrea Doria, I-95129 Catania, Italy

[4)] Nuclear Science Division, Lawrence Berkeley Laboratory
University of California, Berkeley, California 94720, USA

September 30, 1994

Abstract

The numerical simulation of the nuclear Boltzmann-Langevin equation is investigated for idealized two-dimensional nuclear matter. The equivalence of the lattice and test-particle methods are demonstrated for both the mean field evolution, the average collision integral, and the agitation and growth of unstable collective modes for various densities and temperatures.

*This work was supported by the Director, Office of Energy Research, Office of High Energy and Nuclear Physics, Nuclear Physics Division of the U.S. Department of Energy, under Contract No. DE-AC03-76SF00098, and by the Commission of the European Community, under Contract No. ERBCHBI-CT-930619

1 Introduction

Over the past decade, there has been considerable interest in time-dependent nuclear mean-field theory, due in large part to its success in describing many aspects of intermediate-energy nuclear collisions [1]. In particular, the semiclassical version of the time-dependent Hartree-Fock model has been extended by incorporating a Pauli-suppressed collision term, leading to a Boltzmann-like dynamical description [2], often denoted the *BUU* model.[1]

Given the initial one-body phase-space density $f(\boldsymbol{r},\boldsymbol{p},t=0)$, these theories produce a single trajectory for the system in the one-body phase space, $f(\boldsymbol{r},\boldsymbol{p},t)$. Consequently, they cannot provide a description of fluctuations and are therefore inadequate for addressing such phenomena as correlations in light-particle emission, fluctuations of one-body observables, and multifragmentation. In order to obtain a description of fluctuations in the evolution of the nuclear system, a suitable extension of the transport theory is required. In the work of Bixon and Zwanzig [3], a prescription was given for incorporating small-amplitude fluctuations around equilibrium into the Boltzmann equation. However, this method cannot be extended to large-amplitude fluctuations and non-equilibrium scenarios.

A possible extension of the *BUU*-type transport theories was suggested by Ayik and Gregoire [4], consisting of the addition of a stochastic term in the equation of motion for the one-body density. The resulting *Boltzmann-Langevin* equation of motion is then

$$\frac{\partial}{\partial t}f(\boldsymbol{r},\boldsymbol{p},t) = \{h[f],f\} + \bar{I}[f] + \delta I[f]\ . \tag{1}$$

There are thus three distinct sources for the evolution of the one-body density. The first is the collisionless propagation of f in the self-consistent one-body field described by the effective Hamiltonian $h(\boldsymbol{r},\boldsymbol{p})$; this part is often referred to as the Vlasov propagation and corresponds to the *TDHF* description. The second source of evolution is $\bar{I}[f]$ which represents the average effect of the residual two-body collisions; this is the term included in the *BUU*-type descriptions. The third term, $\delta I[f]$, is the new stochastic term and it is ordinarily assumed to represent the fluctuating effect of the two-body collisions. The collision term acts as a Langevin force on the one-body density which then evolves in a manner similar to Brownian motion, giving rise to the term of the Boltzmann-Langevin theory.

In ref. [5] a Fokker-Planck transport formalism was developed for treating the *BL* problem and it offers a convenient formal framework for discussing stochastic one-body dynamics. It has been demonstrated that the Fokker-Planck approach is equivalent to the direct simulation of the *BL* equation [6]. Several applications have been made to fluctuations of one-body observables in nuclear dynamics [6, 7, 8] and it has been demonstrated that the lattice phase-space method (i)

[1] A variety of names have been employed in the literature: Boltzmann-Uehling-Uhlenbeck (*BUU*), Vlasov-Uehling-Uhlenbeck, Landau-Vlasov, or Boltzmann-Nordheim-Vlasov.

produces results that are in very good agreement with expectations based on statistical mechanics, and (*ii*) is able to break symmetries that have been artificially imposed on the initial density, thus making the approach suitable for addressing multifragmentation processes. The purpose of the present paper is to compare this numerical method with the more familiar test-particle method, especially in the presence of instabilities when numerical errors are particularly critical.

The presentation is organized as follows: In sect. 2 we discuss different methods of discretization of the mean field and the collision integral, and we compare the test-particle method with the lattice simulation. In sect. 3 we discuss the growth of instabilities in spinodal nuclear matter, and in sect. 4 we illustrate the propagation and amplification of fluctuations for various densities and temperatures. Finally, sect. 5 presents a concluding discussion.

2 Numerical methods

In the present study we ignore the spin-isospin degrees of freedom of the nucleons for simplicity, since their inclusion would have no bearing on our findings.

2.1 Test-particle method

Boltzmann-like equations can conveniently be solved by means of the so called test-particle method (see, for example, ref. [2]). The basic idea is to represent $f(\boldsymbol{r},\boldsymbol{p},t)$ by a large number of test particles, $\mathcal{N}$,

$$f(\boldsymbol{r},\boldsymbol{p};t) \approx \frac{1}{\mathcal{N}} \sum_{n=1}^{A\mathcal{N}} \delta(\boldsymbol{r}-\boldsymbol{r}_n, \boldsymbol{p}-\boldsymbol{p}_n; t) \; . \tag{2}$$

In order to calculate the Pauli suppression factors $\bar{f} = 1 - f$, it is necessary to have a smooth density in momentum space. In our studies, this is achieved by performing a convolution with a normalized gaussian having a width $\sigma_p = 0.15\ \hbar/\mathrm{fm}$. The collisionless part of the test-particle motion is governed by the newtonian equations of motion implied by the effective Hamiltonian, while the collision integral is treated by a Monte Carlo method based on the specified nucleon-nucleon cross section $\sigma_{NN} \approx 40$ mb [9]. It should be noted that the test-particle method is not intended to present any stochastic behavior. Indeed, the number of test particles per nucleon, $\mathcal{N}$, is merely a numerical parameter that should be chosen sufficiently large to render the results independent of $\mathcal{N}$. However, even for large $\mathcal{N}$, there is always a remaining fluctuation and a finite numerical viscosity associated with the test-particle method, as will be discussed elsewhere [10].

2.2 Lattice method

Spurious fluctuations can be avoided by discretizing the phase space on a lattice, thereby eliminating the need for Monte Carlo evaluations and thus obtained a

truly deterministic evolution. The phase-space is then divided into a cartesian lattice of cells $i \equiv (\alpha, \beta)$, with α and β labeling the lattice sites in position and momentum space, respectively. Each cell has the side lengths Δr and Δp. The corresponding elementary phase-space volume is then $\Delta\Omega = (\Delta r \Delta p/h)^D$, where D is the dimension of the physical space. Most computational problems associated with nuclear Vlasov dynamics arise from the need to have a smooth one-body density, so that derivatives are well behaved. In order to achieve a sufficiently fine paving of the phase-space, the magnitudes of Δr and Δp should be smaller than the range of the nuclear force and the Fermi momentum, respectively. Typically, $\Delta r \leq 1$ fm, while $\Delta p \leq 100$ MeV/c. The discretization introduces a noiseless numerical error on the physical observables, which can be systematically reduced by employing an increasing number of ever smaller cells, so the degree of accuracy that can be obtained is limited only by the storage capability and by the corresponding rapid growth in computing time.

2.2.1 Discretization of the mean field

The discretization of the mean field is not a trivial problem, because conservation of particle number and energy is easily violated. We therefore discuss our adopted method in some detail.

After discretization of the gradients, the total time derivative of the one-body distribution function $f_{\alpha\beta}$ reads, on a one-dimensional grid,

$$\frac{\partial}{\partial t} f_{\alpha\beta} + v_\beta \, \frac{f_{\alpha+1,\beta} - f_{\alpha-1,\beta}}{2\Delta r} + F_\alpha \, \frac{f_{\alpha,\beta+1} - f_{\alpha,\beta-1}}{2\Delta p} = 0 \, . \tag{3}$$

where F_α is the force and v_β the velocity. It is then straightforward to demonstrate that both particle number A, momentum P , and energy E are conserved, to first order in time,

$$\frac{d}{dt} A = \Delta\Omega \sum_{\alpha\beta} \frac{\partial}{\partial t} f_{\alpha\beta} = 0 \, , \tag{4}$$

$$\frac{d}{dt} P = \Delta\Omega \sum_{\alpha\beta} p_\beta \frac{\partial}{\partial t} f_{\alpha\beta} = 0 \, , \tag{5}$$

$$\frac{d}{dt} E = \Delta\Omega \sum_{\alpha\beta} h_{\alpha\beta} \frac{\partial}{\partial t} f_{\alpha\beta} = 0 \, , \tag{6}$$

provided the velocity and the force are given by

$$v_\beta = \frac{\Delta h}{\Delta p} = \frac{p_{\beta+1}^2 - p_{\beta-1}^2}{4m\Delta p} = \frac{p_{\beta+1} + p_{\beta-1}}{2m} = \frac{p_\beta}{m} \, , \tag{7}$$

$$F_\alpha = -\frac{\Delta h}{\Delta r} = -\frac{U_{\alpha+1} - U_{\alpha-1}}{2\Delta r} \, , \tag{8}$$

i.e. the standard lattice representations of the gradients of the Hamiltonian $h_{\alpha\beta}$.

Adopting the above lattice scheme, we solve the Vlasov propagation on the lattice by means of a matrix method. The Vlasov equation then has the form,

$$\|\dot{f}(t) \gg = \mathcal{M}_{\mathbf{r}} \|f(t) \gg + \mathcal{M}_{\mathbf{p}} \|f(t) \gg \tag{9}$$

where f is considered as a supervector denoted $\|f \gg$, and $\mathcal{M}_{\mathbf{r}}$ and $\mathcal{M}_{\mathbf{p}}$ are matrices which can be constructed from the effective field and the momenta, respectively, using Eq. (3). The above equation can then be solved to second order in Δt,

$$\|f(t+2\Delta t) \gg = \frac{1+(\mathcal{M}_{\mathbf{r}}+\mathcal{M}_{\mathbf{p}})\Delta t}{1-(\mathcal{M}_{\mathbf{r}}+\mathcal{M}_{\mathbf{p}})\Delta t} \|f(t) \gg , \tag{10}$$

requiring only the inversion of the matrix $1-(\mathcal{M}_{\mathbf{r}}+\mathcal{M}_{\mathbf{p}})\Delta t$.

It is important to take account of the fact that the propagations in coordinate and momentum space do not commute, due to the position dependence of the force $\mathbf{F}$. Recalling that the self-consistent propagation of classical particles can be accurately solved by the following "leapfrog" algorithm [2],

$$\boldsymbol{r}(t+\Delta t) = \boldsymbol{r}(t-\Delta t) + 2\Delta t \, \frac{\boldsymbol{p}(t)}{m} , \tag{11}$$

$$\boldsymbol{p}(t+2\Delta t) = \boldsymbol{p}(t) + 2\Delta t \mathbf{F}(t+\Delta t) , \tag{12}$$

we adopt the following algorithm,

$$\|f' \gg = \frac{1+\mathcal{M}_{\mathbf{r}}[f_m]\Delta t}{1-\mathcal{M}_{\mathbf{r}}[f_m]\Delta t} \|f_m \gg \tag{13}$$

$$\|f_{m+1} \gg = \frac{1+\mathcal{M}_{\mathbf{p}}[f']\Delta t}{1-\mathcal{M}_{\mathbf{p}}[f']\Delta t} \|f' \gg , \tag{14}$$

which propagates the density f from the time $t_m = 2m\Delta t$ to the subsequent time t_{m+1}, via the intermediate density f'. This method has proved to be numerically very accurate for conserving particle number, momentum, and energy.

2.2.2 Discretization of the collision integral

As already discussed in the introduction, the stochastic collision term is decomposed into an average and a fluctuating part, $I = \bar{I} + \delta I$. The average term expresses the mean rate of collisions from two phase-space elements 1 and 2 into two other phase-space elements $1'$ and $2'$ during a small time interval Δt,

$$\bar{n}_{1,2;1',2'} = f_1 f_2 \bar{f}_{1'} \bar{f}_{2'} \; \delta(\boldsymbol{r}_{12}) \delta(\boldsymbol{r}_{1'2'}) \delta(\boldsymbol{r}_{11'}) \; \omega(1,2;1',2') \; \Delta\Omega\Delta t \; . \tag{15}$$

Here f_i is the average value of f over the cell i and the Pauli suppression factor $\bar{f}_i = 1 - f_i$ is the corresponding availability. The average collision integral $\bar{I}$ is obtained by adding all possible elementary contributions $\bar{n}_{1,2;1',2'}$. The transition rate for an elementary scattering process, ω, is related to the differential

cross-section of the colliding nucleons, $d\sigma_{NN}/d\Omega$, which has been assumed to be independent of angle and energy.

The numerical algorithm adopted for calculating the transition rate needs some care. Indeed, in the Boltzmann equation the collisions are assumed to be local in space, implying that the system may be described on scales smaller than that defined by the collision cross-section, as is in fact needed for obtaining a reliable mean-field propagation. In order to have an algorithm that is as independent as possible of the actual coarse graining of the phase space, we have adopted the following procedure. The nucleons in a given cell are allowed to interact with those situated in a given number of neighboring cells. The side length of the corresponding cube, $d_0 = n_c \Delta r$, is taken to be near the interaction range implied by the actual nucleon-nucleon cross section, σ_{NN}. All the nucleons included in the n_c^D cells interact with the nucleons of the considered cell, with a constant collision length λ that has been determined so that the total nucleon-nucleon collision cross section is preserved. The transition rate into a given final state $1'2'$ is then calculated by requiring energy and momentum conservation, and by assuming that the particles remain at the same position in space. It is convenient to pre-calculate and store the transition rate $\omega(1,2;1',2')$.

For convenience, we use a collisional time step that is larger than thoat used for the mean-field propagation. We note that, in contrast with the test-particle method, the lattice method yields the Pauli blocking without numerical noise, since the occupancies are known at each lattice site.

2.2.3 Treatment of the Langevin term

Since the elementary collisions are regarded as independent random processes, the collision number $n_{1,2;1',2'}$ can be regarded as having a Poisson distribution,

$$\sigma_n^2 = \bar{n} \tag{16}$$

Consequently, the stochastic term δI can be produced by adding to the mean value $\bar{n}_{1,2;1',2'}$ a fluctuation $\delta n_{1,2;1',2'}$ chosen randomly from a distribution with a variance equal to $\bar{n}$ (and vanishing mean value). It has been shown that the results are not sensitive to the particular form of the probability distribution employed [11], and therefore we use a normal distribution which is numerically more tractable. Since the number of collisions occurring during the small time interval Δt for a specific elementary process $12 \rightarrow 1'2'$ is usually considerably smaller than unity, the fluctuating part δn dominates over the mean value $\bar{n}$. Special care must then be taken to prevent the dynamical density $f^{(n)}$ from acquiring unphysical values (*i.e.* $f < 0$ which is not allowed in a semiclassical approximation or $f > 1$ which is forbidden by the Pauli exclusion principle).

A reasonable treatment can be obtained by accumulating the fluctuations over a phase-space volume of magnitude h^D, corresponding to an entire nucleon [6]. This is a reasonable method because the fluctuations in the BL treatment arise from the basic physical fact that each elementary collision involves two entire nucleons. Therefore, we carry two different scales in the calculation, the

basic scale used for computing the mean-field evolution and the average collision rate, and a larger scale used for calculating the fluctuations. It is important to match these scales correctly. Given four of the large cells, I, J, I', J', we consider elementary transitions of the form $ij \rightarrow i'j'$, with $i \in I$, $j \in J$, $i' \in I'$, and $j' \in J'$. For each such type of transition, the actual number occurring is

$$n_{i,j;i',j'} = \bar{n}_{i,j;i',j'} + \delta n_{i,j,i',j'} \ , \tag{17}$$

where the mean $\bar{n}_{i,j,i',j'}$ is evaluated as explained above. The total rate of all such transitions is then given by

$$N_{I,J;I',J'} = \bar{N}_{I,J;I',J'} + \delta N_{I,J;I',J'} \ , \tag{18}$$

where $\bar{N}_{I,J;I',J'} = \sum_{i,j,i',j'} \bar{n}_{i,j,i',j'}$. On the basis of $\bar{N}_{I,J;I',J'}$, the fluctuation $\delta N_{I,J;I',J'}$ may now be calculated using eq. (16). Subsequently, the fluctuating part of each of the basic transitions, $\delta n_{i,j,i',j'}$ is obtained by sharing $\delta N_{I,J;I',J'}$ in proportion to the mean rates,

$$\delta n_{i,j,i',j'} = \frac{\bar{n}_{i,j,i',j'}}{\bar{N}_{I,J;I',J'}} \, \delta N_{I,J;I',J'} \ . \tag{19}$$

This method preserves the relation between mean and variance on the large scale, while correlating the fluctuations on the small scale, thus avoiding the inherent diverging behavior as the small scale is reduced. The scheme also has the advantage that the Vlasov propagation and the collision term are computed on the same small scale, thus ensuring high accuracy.

3 Test of the dynamical simulation methods

In order to get a better understanding of the transport equations, it is instructive to compare the test-particle and the lattice simulation methods both for the collision term and the mean field propagation.

3.1 Test of the collision term

For this purpose, we have studied a two-dimensional fermion gas in a constant effective field. We may then employ a single spatial cell, with periodic boundary conditions. The initial momentum distribution has been chosen to be two touching Fermi spheres of radius $P_F = 275$ MeV/c. The lattice size in momentum space is $\Delta p_x = \Delta p_y = 50$ MeV/c and the entire lattice consists of 29×29 momentum cells. The nucleon-nucleon "cross section" was taken as 2.4 fm, corresponding to an interaction range of 1.2 fm. The time step was chosen equal to $\Delta t = 2$ fm/c. The equations of motion were then followed numerically until approximate stationarity was reached.

The corresponding density is shown in fig. 1, with the histogram indicating the lattice result and the solid line being the test-particle result. For reference,

the dashed line shows the associated Fermi-Dirac equilibrium distribution,

$$f^0(\boldsymbol{p}) = [1 + e^{(\frac{p^2}{2m}-\mu)/T}]^{-1} , \tag{20}$$

where $\mu = 62.6$ MeV and $T = 31.6$ MeV are determined by the specified intial density $f(\boldsymbol{p}, t)$. The excellent agreement among all three results gives us confidence in the numerical methods for treating the collision integral.

As a further check, fig. 2 displays the time evolution of the anisotropy, as measured by the quadrupole moment of the momentum distribution,

$$Q = \frac{\int dp_x dp_y (p_x^2 - p_y^2) f(p_x, p_y)}{\int dp_x dp_y (p_x^2 + p_y^2) f(p_x, p_y)} . \tag{21}$$

The solid line is the lattice result, while the dashed line is the test-particle result. The anisotropy relaxes in the same manner in the two approaches, with a relaxation time approximately equal to 9 fm/c [6]. The agreement between the two numerical approaches can also be seen in table 1, which shows the total number of collisions in one single time step for Fermi-Dirac distributions at different temperatures. The result of a direct numerical evaluation of the collision number is also shown. We note that the number of collisions increases with the temperature, as it should be because of the partial relaxation of the Pauli blocking. Moreover, the increase is approximately quadratic in T, as expected [12, 13].

3.2 Test of the mean field propagation

In this section we discuss how the mean field propagates, both in the lattice and test-particle method. In particular, we analyze the behavior of nuclear matter in the spinodal zone of the phase diagram where uniform matter is unconditionally unstable against density fluctuations. We consider again a two-dimensional periodic box and use side lengths $L_x = 63$ fm and $L_y = 21$ fm. For the effective one-body field we employ a simplified Skyrme interaction [8],

$$U(x) = A\frac{\bar{\rho}(x)}{\rho_s} + B(\frac{\bar{\rho}(x)}{\rho_s})^2 , \tag{22}$$

with $A = -100.3$ MeV and $B = 48$ MeV. The saturation density $\rho_s = 0.55$ fm^{-2} corresponds to a Fermi momentum of $p_F = 260$ MeV/c. Furthermore, $\bar{\rho}(x)$ is the local average of the density with respect to the transverse direction y, smeared in the x direction with a gaussian of width $\sigma_r = 0.87$ fm. It should be noticed that in the case of the lattice calculation the lattice is introducing an additional smearing and therefore the gaussian width must be correspondingly reduced in order to compensate from this effect.

Since we wish to study the behavior of the system in the spinodal region, the initial conditions are chosen as a uniform density ρ_0 equal to half the saturation density ρ_s and having a finite temperature equal to $T = 3$ MeV, which places the system near the center of the spinodal region [14].

In order to achieve a better understanding of the instabilities, we first consider the linearized Vlasov equation at zero temperature. The resulting dispersion relation is easy to derive [14] and for unstable systems it reads,

$$\frac{\hbar}{t_k^{\mathrm{mf}}} = k\left(\frac{\epsilon_0}{\rho_0} + \frac{\partial U}{\partial \rho}\mathrm{e}^{-k^2a^2/2}\right)\left[-\frac{m}{\rho}\left(\frac{\epsilon_0}{2\rho_0} + \frac{\partial U}{\partial \rho}\mathrm{e}^{-k^2a^2/2}\right)\right]^{-\frac{1}{2}}, \tag{23}$$

where $a = \sigma_r/\hbar$, k is the wave number of the unstable mode and ϵ_0 is the Fermi energy associated with the specified initial density ρ_0. The partial derivatives of the mean field are calculated at the actual density.

In order to extract the actual dispersion relation from the numerical simulations, we have considered a slight harmonic perturbation on the initial uniform density along the x direction. For each perturbation characterized by the wave number k, we have performed a pure Vlasov evolution and determined the growth time t_k from the growth of the Fourier component of $\bar{\rho}(x)$ corresponding to the wave number k. It has of course been verified that the linear response theory remains valid during the time needed to accurately compute the growth time, by checking that the Fourier components associated with the wave number different from the considered k were not becoming important and by confirming that the growth of the component associated with k was actually exponential. It was found that most of the exponential growth persists up to about 75 fm/c, after which time fragments are so well developed that the linear response treatment no longer applies.

Figure 3 displays the solutions to eq. (23). The stars and the circles represent the results obtained in the lattice and test-particle method, respectively. We note a quite good agreement between the analytical result (23) and the numerical simulations. The small differences between the two methods will be discussed in the next section.

Of course, the complete dispersion relation must take into account collisional and temperature effects. For small temperatures, the dependence on T s only slight and so may be ignored. As for the effect of the two-body collisions, their contribution has been shown to be rather negligible, within the relaxation-time approximation [15, 16].

4 Test of unstable collective dynamics

We now turn to the self-consistent dynamics of the unstable collective modes. When considering such catastrophic processes, it is especially important to analyze how fluctuations are propagated by the unstable effective field. In order to establish a useful reference, we first present a brief summary of the analysis made in ref. [14].

4.1 Linear Vlasov propagation of fluctuations

In an infinite system the collective modes are plane waves, and so it is helpful to perform a Fourier analysis of the density fluctuations for the considered ensemble,

$$\sigma_k(t) = \prec |\rho_{\mathbf{k}}(t)|^2 \succ = \int\int dx dx' \; \mathrm{e}^{-ik(x-x')} \; \prec \delta\rho(x,t) \; \delta\rho(x',t) \succ \; . \tag{24}$$

where $\delta\rho(x) = \bar{\rho}(x) - \rho_0$ represents the fluctuating part of the matter density. Following refs. [8, 14], we linearize the problem and concentrate on the collective part of the response. Since there is a growing and a decaying eigenmode for each wave number (labeled by the superscript $\nu = \pm$), the above variance consists of four terms, $\sigma_k = \sum_{\nu\nu'} \sigma_k^{\nu\nu'}$, each governed by a simple feedback equation of motion,

$$\frac{d}{dt}\sigma_k^{\nu\nu'}(t) = 2\mathcal{D}_k^{\nu\nu'} + \frac{\nu+\nu'}{t_k} \; \sigma_k^{\nu\nu'}(t) \; . \tag{25}$$

Here $\mathcal{D}_k^{\nu\nu'}$ denotes the corresponding source term arising from the stochastic part of the collision integral, and the feedback arises from the response of the effective field, in accordance with the dispersion relation (23). These four equations can readily be solved analytically and the resulting time development for the variance coefficient σ_k is then given by

$$\sigma_k(t) = 2\mathcal{D}_k^{++} t_k \sinh(\frac{2t}{t_k}) + 4\mathcal{D}_k^{+-} t + 2\sigma_k^{++}(0) \; \sinh(\frac{2t}{t_k}) + 2\sigma_k^{+-}(0) \; , \tag{26}$$

Here $\sigma_k^{\nu\nu'}(0)$ denotes the initial fluctuations, appropriately projected, which was assumed to fulfil the relation and $\sigma_k^{++}(0) = \sigma_k^{--}(0)$. We have also utilized that $\mathcal{D}_k^{++} = \mathcal{D}_k^{--}$ and $\mathcal{D}_k^{+-} = \mathcal{D}_k^{-+}$. It is thus clear that the presence of an instability will soon lead to an exponential growth of the corresponding variance σ_k.

4.2 Fluctuations induced by the numerical methods

In order to be able to treat the stochastic evolution correctly, we must first fully understand the possible sources of fluctuation arising from the discretization procedures.

In the case of the lattice simulations, we have checked that initially uniform unstable matter does not evolve at all, in the absence of the stochastic part of the collision term δI. This is due to the fact that no part of the Vlasov propagation algorithm is able to break the initial translational symmetry and because the effect of the average collision term $\bar{I}$ is completely deterministic in the lattice treatment. This demonstrates that the lattice method does not introduce additional fluctuations and so it provides a safe basis for treating stochastic dynamics.

The situation is quite different in the test-particle method. Indeed, the finite value of $\mathcal{N}$ introduces fluctuations already in the initial state. This initial fluctuation is simple to calculate [17],

$$\sigma_k = \frac{L_x}{L_y}\frac{\rho}{\mathcal{N}} \; , \tag{27}$$

corresponding to a white noise spectrum (*i.e.* σ_k is independent on the wave number k).

In addition, the test-particle simulation also generates fluctuations in the dynamics, both from the Monte-Carlo estimation of the collision term and from the propagation of the test particles [10].

As far as the average collision term is concerned, it is clear that the Monte-Carlo estimation in effect acts as a stochastic collision term, due to the finite value of $\mathcal{N}$. Indeed, the contribution from $\bar{I}$ is completely analogous to the source term $\mathcal{D}_k$ of the Boltzmann-Langevin theory, except that is must be divided by $\mathcal{N}$.

Finally, since we are treating a gas of classical particles (the only quantum effect is the Pauli blocking in the collision integral), the calculations also contain fluctuations and correlations associated with the disordered propagation of the test particles in the effective field. So even if the initial fluctuations were artificially put to zero, density fluctuations will be generated as a result of the Vlasov propagation. In fact, the simulation is equivalent to molecular dynamics for the test particles and so it contains many-body correlations at this level [10, 18]. These correlations provide an additional source of fluctuation which can be calculated as a function of the density and the temperature of the system [10]. When $\mathcal{N}$ is increased, most of these effects diminish as powers of $1/\mathcal{N}$. However, even in the limit of very large $\mathcal{N}$, a constant numerical viscosity on the one-body dynamics will remain [10].

Since disturbances are so quickly amplified in the spinodal zone no matter how large is $1/\mathcal{N}$ the numerical fluctuation will soon generate large fluctuations. Indeed, if we look at the asymptotic evolution, it follows from eq. (26) that the magnitude of the fluctuations is given by $\sigma_k^{++}(0)+\mathcal{A}_k^{++}t_k$ in the BUU test-particle simulation. We have then performed BUU calculations using a range of values for $\mathcal{N}$. The time evolution of the fastest mode is shown in fig. 4 for two different test-particle numbers. The time evolutions follow the form given in eq. (26) which are also displayed in fig. 4. This confirms the $1/\mathcal{N}$ scaling.

Figure 5a shows the evolution of one particular density distribution (calculated in the test-particle method with $\mathcal{N} = 90$), while fig. 5b presents the fluctuation σ_k computed over an ensemble containing 100 events. It is clear that the density irregularities quickly attain a sizable magnitude.

This clearly demonstrates that any Langevin dynamics based on the test-particle method must be performed with a much larger number $\mathcal{N}$, at least several thousand, in order to have results which are not dominated by numerical noise. However, as far as spinodal instabilities are concerned, it has been suggested and explored in ref. [17] that the numerical noise of the test-particle method can be used as a fluctuation source in order to have a very schematic Langevin dynamics. Indeed, the noise of the test-particle method can be tuned by employing a suitable number of test particles $\mathcal{N}$ in order to mimic the behaviour of the most unstable mode found in the BL dynamics. In the present case the value $\mathcal{N} = 90$ is predicted to achieve the above requirement and indeed we observe that figs. 4 and 5 are remarkably similar to the prediction of the BL simulations (figs. 6 and 7. However, we would like to stress that this ultra-simplified Langevin dynamics

based on the noise induced by the finite sampling of the phase space is very crude an approximation which can only give qualitative answers when real collisions are considered. Therefore, in order to become really quantitative, better methods are clearly called for [19].

4.3 Lattice simulation of BL dynamics

Let us now turn to the study of the exact Boltzmann-Langevin dynamics performed on the lattice. We have used basic lattice spacings of $\delta x = \frac{1}{3}$ fm and $\delta p = 40$ MeV/c which gives a fairly good phase-space paving resolution.

We first focus on the evolution of the spatial density of the system, which is displayed in fig. 7a. Initially the system has a uniform density, but soon the fluctuations break this translational symmetry. Subsequently the fluctuations are rapidly amplified by the action of the effective one-body field, thus leading towards fragment formation.

Figure 7b displays the coefficient σ_k as a function of the node number $K = kL/2\pi$. It can be seen that certain modes are amplified more rapidly than others, in accordance with their respective characteristic times t_k, and the final Fourier spectrum is therefore dominated by the most unstable modes. Eq. (26) provides a good understanding of the growth of the fluctuations. In fact, at early times, the fluctuation coefficient reflects the spectrum of the initial noise and it grows linearly in time as the collective modes are agitated by the respective source terms. Subsequently, the instabilities start to manifest themselves and the rise becomes purely exponential. At still later times, beyond the linear regime, fragments begin to form and $\sigma_k(t)$ levels off.

In order to better elucidate the dynamics in the spinodal zone, it is instructive to exhibit the dependence of the diffusion coefficient and the instability growth times on the initial density and temperature. For that, we studied an ensemble of 50 events for a density-temperature grid within the spinodal zone of our two-dimensional test system. The spectral analysis of the fluctuations provides the values of the source terms and the growth times. A typical fit using by eq. (26) is displayed in fig. 6 (squares) for a given point well inside the spinodal zone. We obtain $\mathcal{D}_k = 1.6 \cdot 10^{-3}$ c/fm^3 for the source term and $t_k = 38$ fm/c for the growth time. These values agree well with those obtained analytically in ref. [14] for $\mathcal{D}_k$. Systematic comparisons are shown in figs. 8 and 9. The dashed lines represent the numerical BL lattice simulation, while the solid lines are analytical results obtained directly from the linear response theory for unstable systems [14]. (When making the comparison between the BL lattice simulations and the linear-response treatment, one should keep in mind that the method employed in ref. [14] is only approximate, so perfect agreement should not be expected; a more refined method is presently being developed [20].) The dependence on the temperature is stronger than on the density, as expected since the source term D_k is closely related to the rate of collisions in by the system [14], and this number is proportional to T^2 and $\sqrt{\rho}$ in $2D$. In fig. 9 we show the extracted growth times. The dependence of the growth time t_k on temperature and density is weaker than

for the diffusion coefficient, as one would also expect from simple considerations [16].

5 Conclusion

In this paper we have shown how it is possible to describe catastrophic evolutions of nuclear matter within the nuclear Boltzmann transport theory, using a lattice method. The equivalence between this method and the more common test-particle method was demonstrated regarding the average one-body dynamics. The numerical errors and possible noise of the two methods are discussed. The lattice treatment was then extended to incorporate the Langevin fluctuation term and we showed that the resulting approach is reliable for describing processes in which fluctuations play a decisive role, such as is expected in multifragmentation events. The *BL* model allows one to include both the stochastic collisions, which create the seeds for the density fluctuations, and the effective field, which propagates and amplifies them, thus leading the system towards fragmentation. We have shown how the early evolution can be quantitatively understood within linear response theory, with a dispersion relation that predicts the growth of instabilities to good accuracy. The dependence of the source terms on density and temperature was also briefly illustrated.

This exposition complements earlier presentations and is intended to provide a better understanding of both the lattice method and the test-particle method, as well as their mutual relationship.

Acknowledgements: We thank M. Di Toro (LNS-Catania), A. Bonasera (LNS-Catania), A. Guarnera (Ganil-LNS), and F. Gulminelli (INFN-Milano) for fruitful discussions, and we also wish to acknowledge the stimulating role played by P. Fox (Downtown Caen). This work was supported by the Director, Office of Energy Research, Office of High Energy and Nuclear Physics, Nuclear Physics Division of the U.S. Department of Energy, under Contract No. DE-AC03-76SF00098, and by the Commission of the European Community, under contract No. ERBCHBI-CT-930619. Two of us (GFB & JR) wish to acknowledge support and hospitality by the National Institute for Nuclear Theory at the University of Washington, Seattle, where this work was completed.

References

[1] P. Schuck, R.W. Hasse, J. Jaenicke, C. Gregoire, B. Remaud, F. Sebille, and E. Suraud, Prog. Part. Nucl. Phys. 22 (1989) 181;
W. Cassing, V. Metag, U. Mosel, and K. Niita, Phys. Rep. 188 (1990) 363

[2] G.F. Bertsch and S. Das Gupta, Phys. Rep. 160 (1988) 190; J. Aichelin and G.F. Bertsch, Phys. Rev. C31 (1985) 1730;

H. Kruse, B. Jacak, and H. Stöcker, Phys. Rev. Lett. 54 (1985) 289;

C. Gregoire, B. Remaud, F. Sebille, L. Vinet and Y. Raffray, Nucl. Phys. A465 (1987) 317

[3] M. Bixon and R. Zwanzig, Phys. Rev. 187 (1969) 267

[4] S. Ayik and C. Gregoire, Phys. Lett. B212 (1988) 269; Nucl. Phys. A513 (1990) 187

[5] J. Randrup and B. Remaud, Nucl. Phys. A514 (1990) 339

[6] F. Chapelle, G.F. Burgio, Ph. Chomaz, and J. Randrup, Nucl. Phys. A540 (1992) 227

[7] Ph. Chomaz, G.F. Burgio, and J. Randrup, Phys. Lett. B254 (1991) 340; G.F. Burgio, Ph. Chomaz, and J. Randrup, Nucl. Phys. A529 (1991) 157

[8] G.F. Burgio, Ph. Chomaz and J. Randrup, Phys. Rev. Lett. 69 (1992) 885

[9] A. Bonasera, G.F. Burgio, and M. Di Toro, Phys. Lett. B221 (1989) 233

[10] Ph. Chomaz and M. Colonna, in preparation

[11] J. Randrup, Nucl. Phys. A545 (1992) 47c

[12] G.F. Bertsch, Z. Phys. A 289 (1978) 103

[13] J. Randrup and S. Ayik, Nucl. Phys. 572 (1994) 489

[14] M. Colonna, Ph. Chomaz, and J. Randrup, Nucl. Phys. A567 (1994) 637

[15] H. Heiselberg, C.J. Pethick, and D.G. Ravenhall, Ann. Phys. 223 (1993) 37

[16] J. Randrup, LBL-35848 (1994), in preparation

[17] M. Colonna, G.F. Burgio, Ph. Chomaz, M. Di Toro, and J. Randrup, Phys. Rev. C47 (1993) 1395

[18] P.G. Reinhardt and E. Suraud, private communication (1994)

[19] Ph. Chomaz, M. Colonna, A. Guarnera, and J. Randrup, LBL-35988 (1994), subm. to Phys. Rev. Lett.

[20] S. Ayik, Ph. Chomaz, M. Colonna, and J. Randrup, in preparation

Table 1: Collision rates.

T (MeV)	Exact	Lattice	Test particles
3	2.23	2.59	3.73
4	4.29	4.61	6.02
5	7.20	7.74	8.62
6	11.14	11.98	11.74

The total rate of nucleon-nucleon collisions at normal density, for a Fermi-Dirac distribution prepared at a given temperature T, as obtained by either a direct numerical evaluation of the collision integral, or with the lattice and test-particle dynamical simulations.

Figure 1:
The calculated stationary one-body density f, as a function of the momentum p, resulting from an initial configuration consisting of two touching Fermi spheres. Solid histogram: lattice simulation. Solid curve: test-particle simulation. Dashed curve: the Fermi-Dirac distribution corresponding to the specified density and energy.

Figure 2:
The relaxation of the anisotropy Q obtained when starting from the same initial configuration as in fig. 1, calculated with either the lattice simulation (solid) or the test-particle method (dashed).

Figure 3:
The growth rate of instabilities, t_k^{-1} as a function of the wave number k, obtained from either the dispersion relation (23) (dashed curve), or with the lattice (stars) and test-particle (circles) simulations. The error bars indicate the uncertainties associted with extracting the rate of the exponential growth rates.

Figure 4:
The fluctuation coefficient σ_k as a function of time, for the mode having $k = 0.6$ fm^{-1}, as obtained with either $\mathcal{N} = 500$ (lower) or $\mathcal{N} = 90$ (upper) test particles per nucleon. The dashed curves represent fits based on eq. (21).

Figure 5:
5*a*: The density profiles of one event, as a function of the position x and at different times t. 5*b*: The fluctuation coefficient σ_k extracted from 100 events, as a function of the node number $K = kL/2\pi$ for the same points in time. The simulations have been performed using $\mathcal{N} = 90$ test particles, at half the saturation density and for $T = 3$ MeV.

Figure 6:
The fluctuation coefficient σ_k vs. time for the most unstable mode ($k = 0.6$ fm^{-1}). The stars represent the lattice simulation, while the dashed curve is a fit of the lattice calculation based on eq. (2).

Figure 7:
Similar to fig. 5, but obtained with the lattice simulation.

Figure 8:
The source term $\mathcal{D}_k$ vs. the initial density for the mode with wave number $k = 0.6$ fm^{-1}, as obtained by either a direct numerical evaluation (solid) or extracted from the lattice simulations (dashed), for the temperatures $T = 1.5$ MeV (diamonds), $T = 3$ MeV (squares), $T = 6$ MeV (circles).

Figure 9:
Similar to fig. 8, for the corresponding growth time t_k.

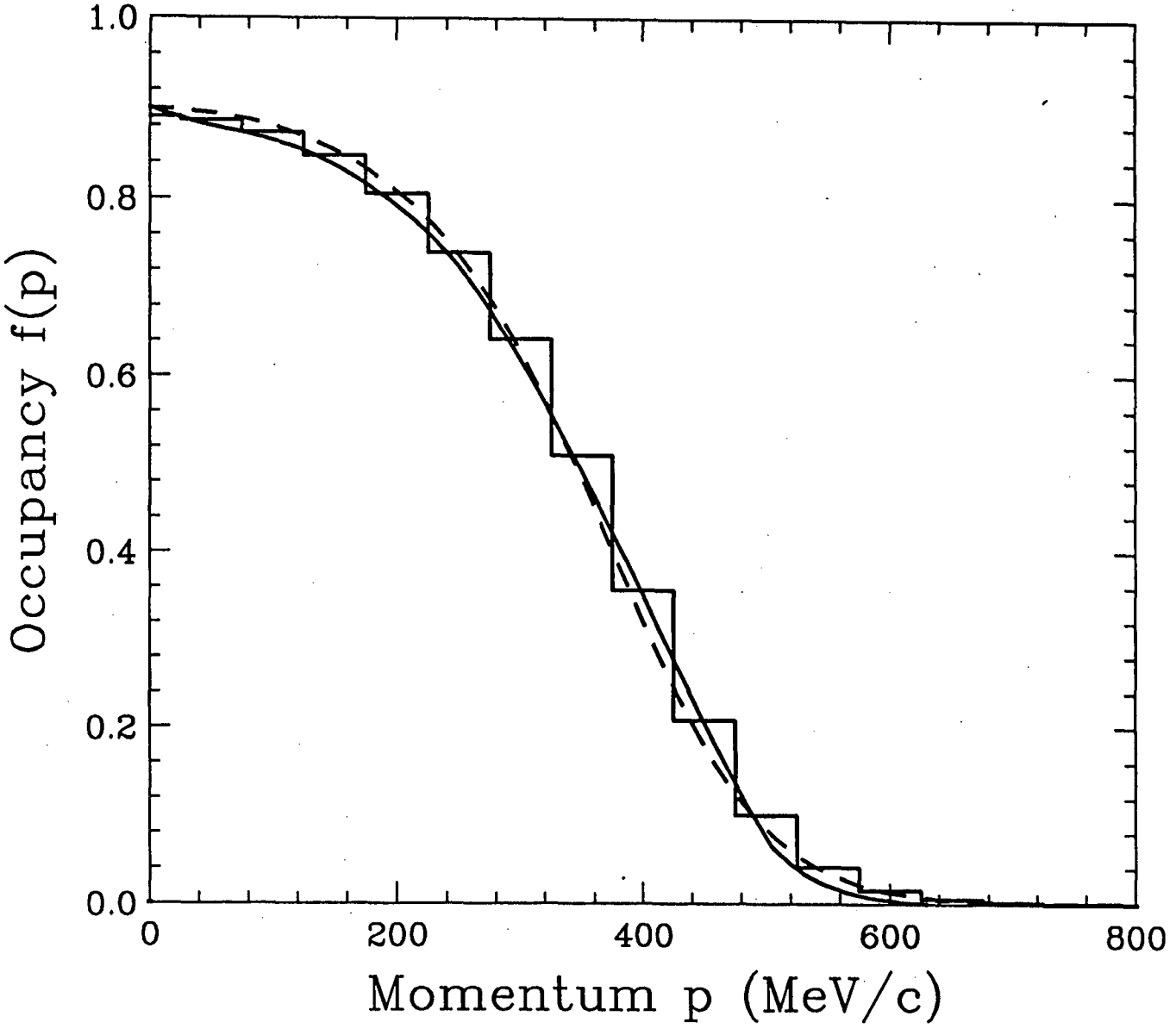

Figure 1

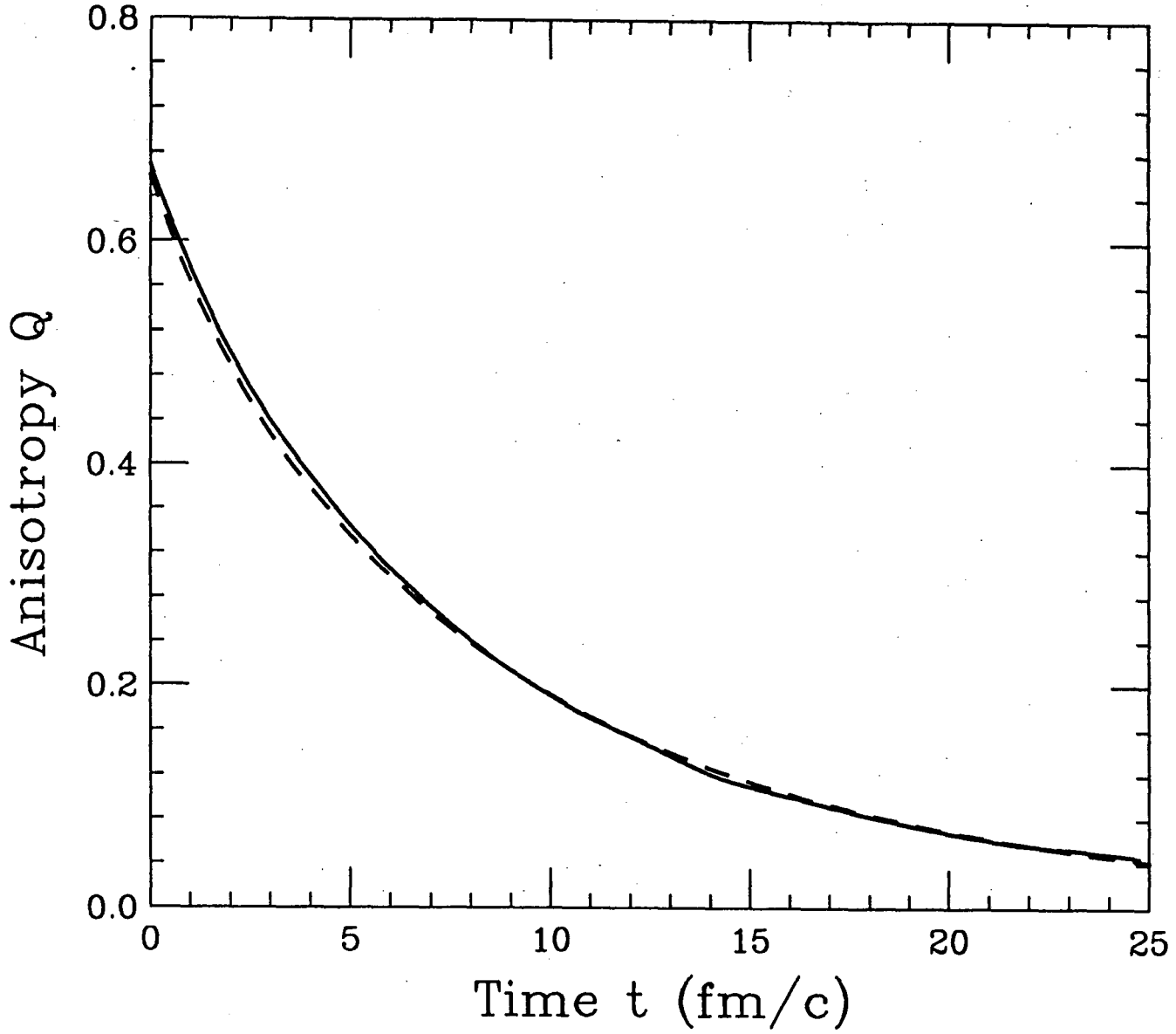

Figure 2

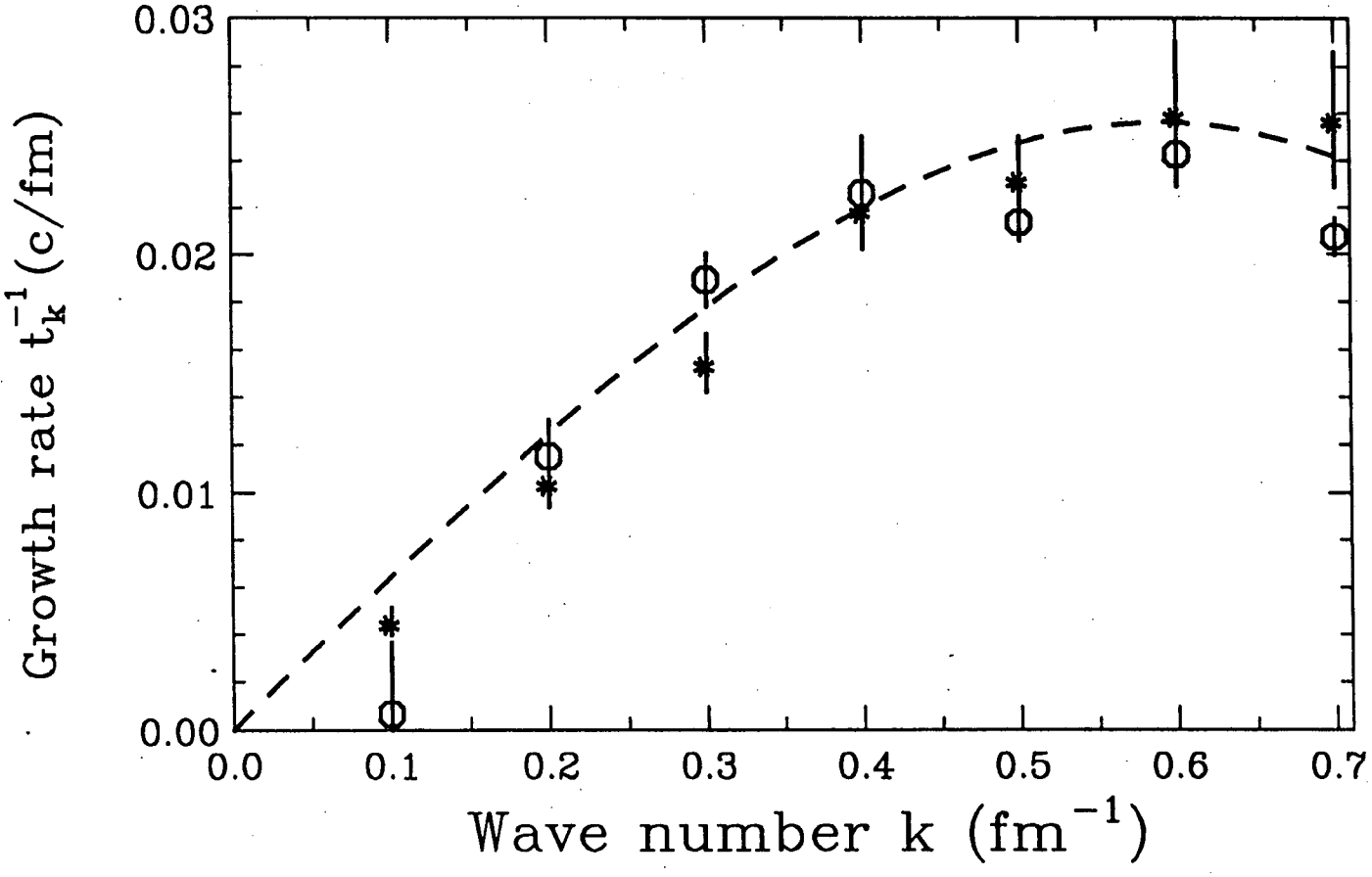
0.03
0.02
0.01
0.00
0.0
0.1
0.2
0.3
0.4
0.5
0.6
0.7
Growth rate t_k^{-1} (c/fm)
Wave number k (fm^{-1})

Figure 3

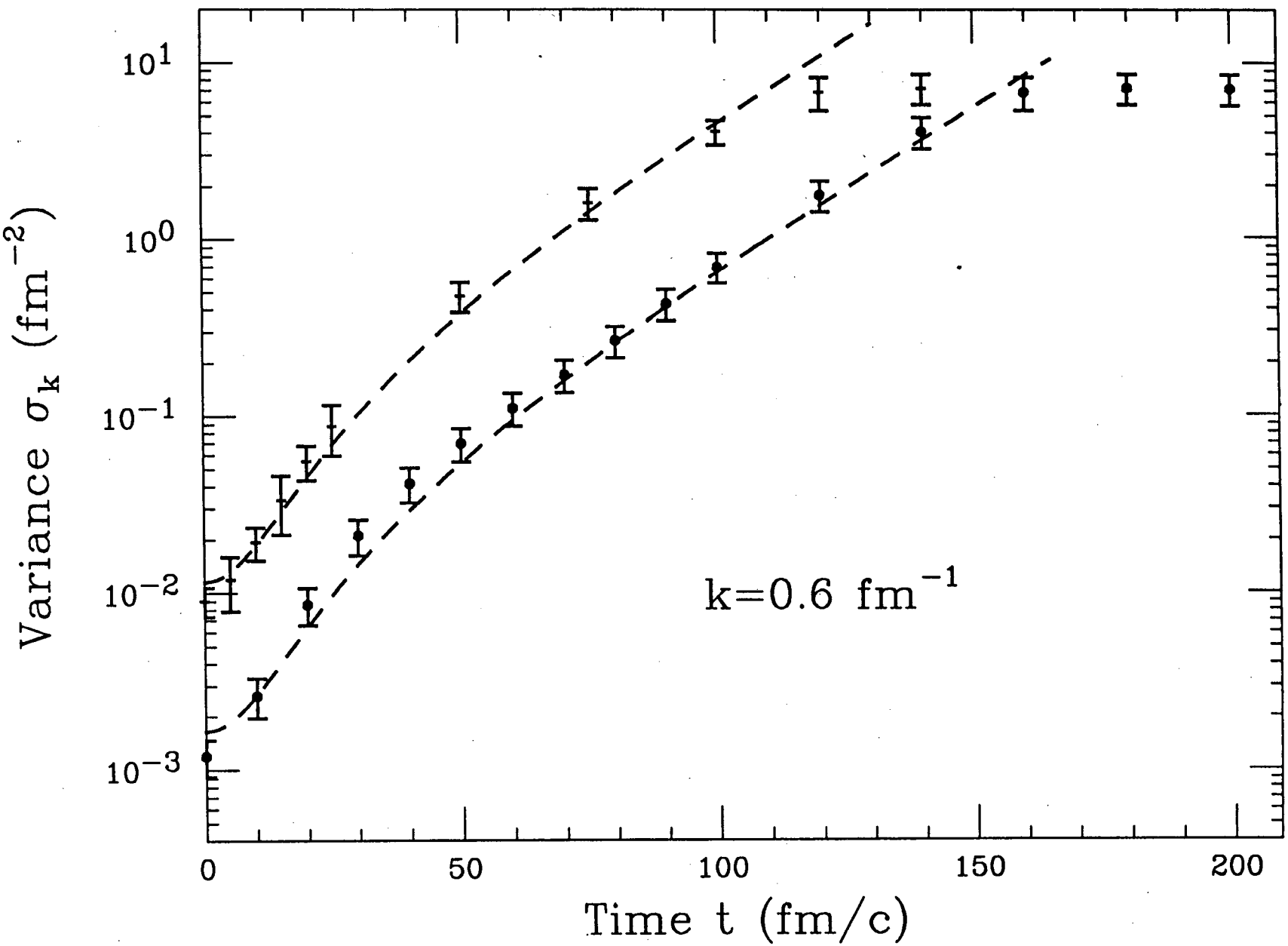
Variance σ_k (fm^{-2})
10^1
10^0
10^{-1}
10^{-2}
10^{-3}
k=0.6 fm^{-1}
0
50
100
150
200
Time t (fm/c)

Figure 4

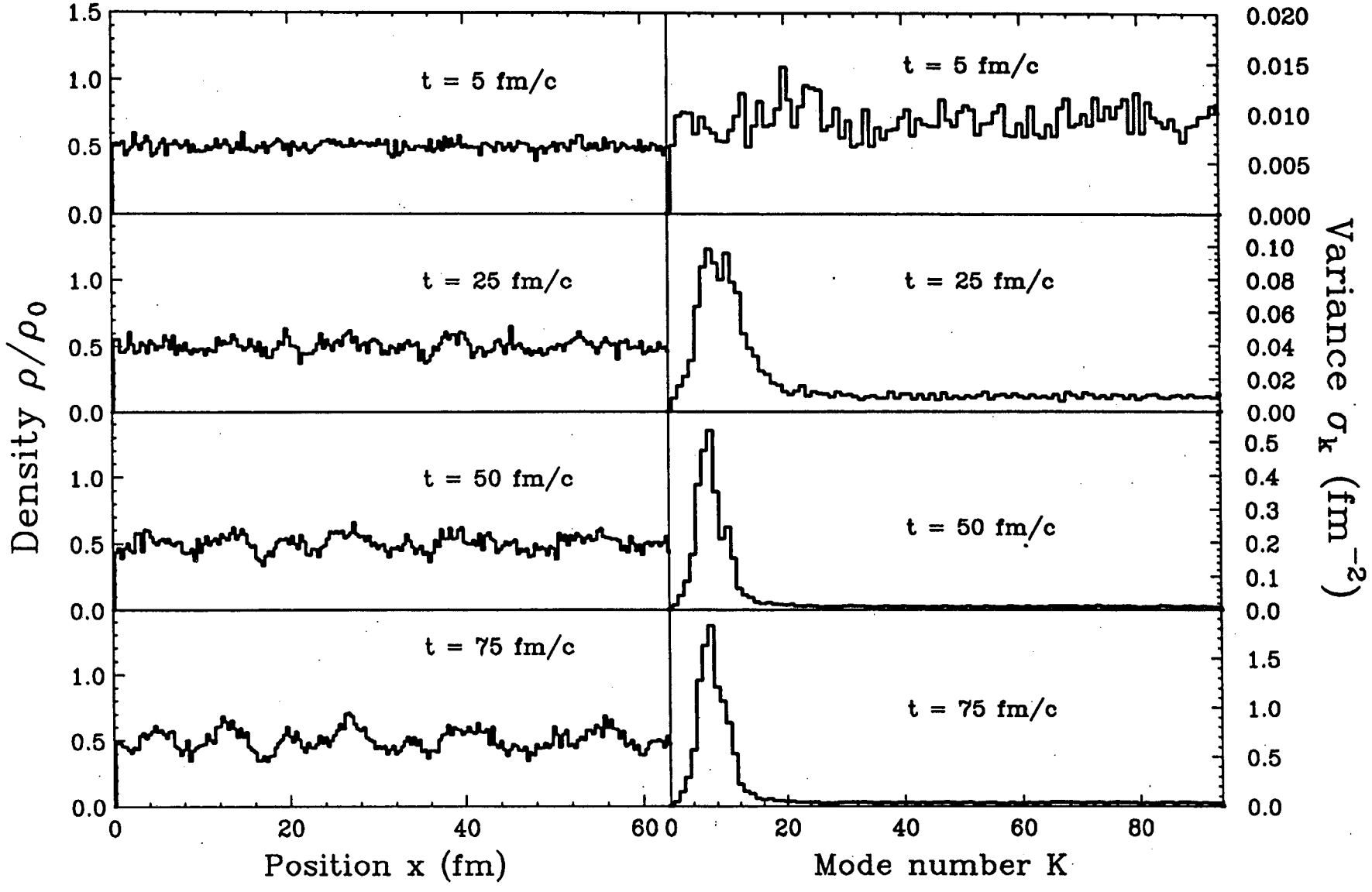
Density ρ/ρ_0
Position x (fm)
Mode number K
Variance σ_k (fm^{-2})
t = 5 fm/c
t = 25 fm/c
t = 50 fm/c
t = 75 fm/c
0.0
0.5
1.0
1.5
0
20
40
60
80
0.000
0.005
0.010
0.015
0.020
0.00
0.02
0.04
0.06
0.08
0.10
0.1
0.2
0.3
0.4
0.5

Figure 5

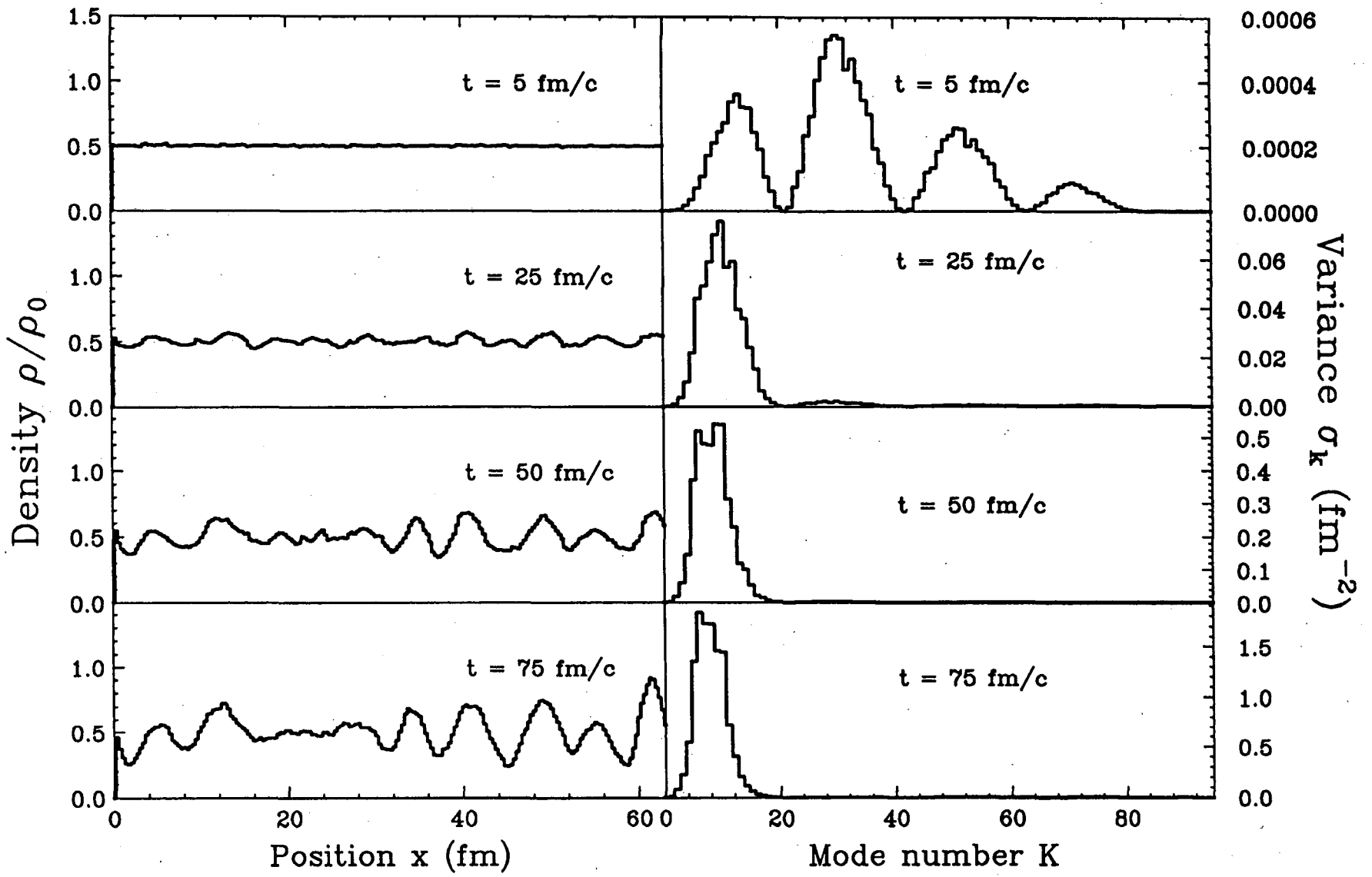
Density ρ/ρ_0
Variance σ_k (fm^{-2})
Position x (fm)
Mode number K
t = 5 fm/c
t = 25 fm/c
t = 50 fm/c
t = 75 fm/c
1.5
1.0
0.5
0.0
0
20
40
60
80
0.0006
0.0004
0.0002
0.0000
0.06
0.04
0.02
0.00
0.5
0.4
0.3
0.2
0.1

Figure 6

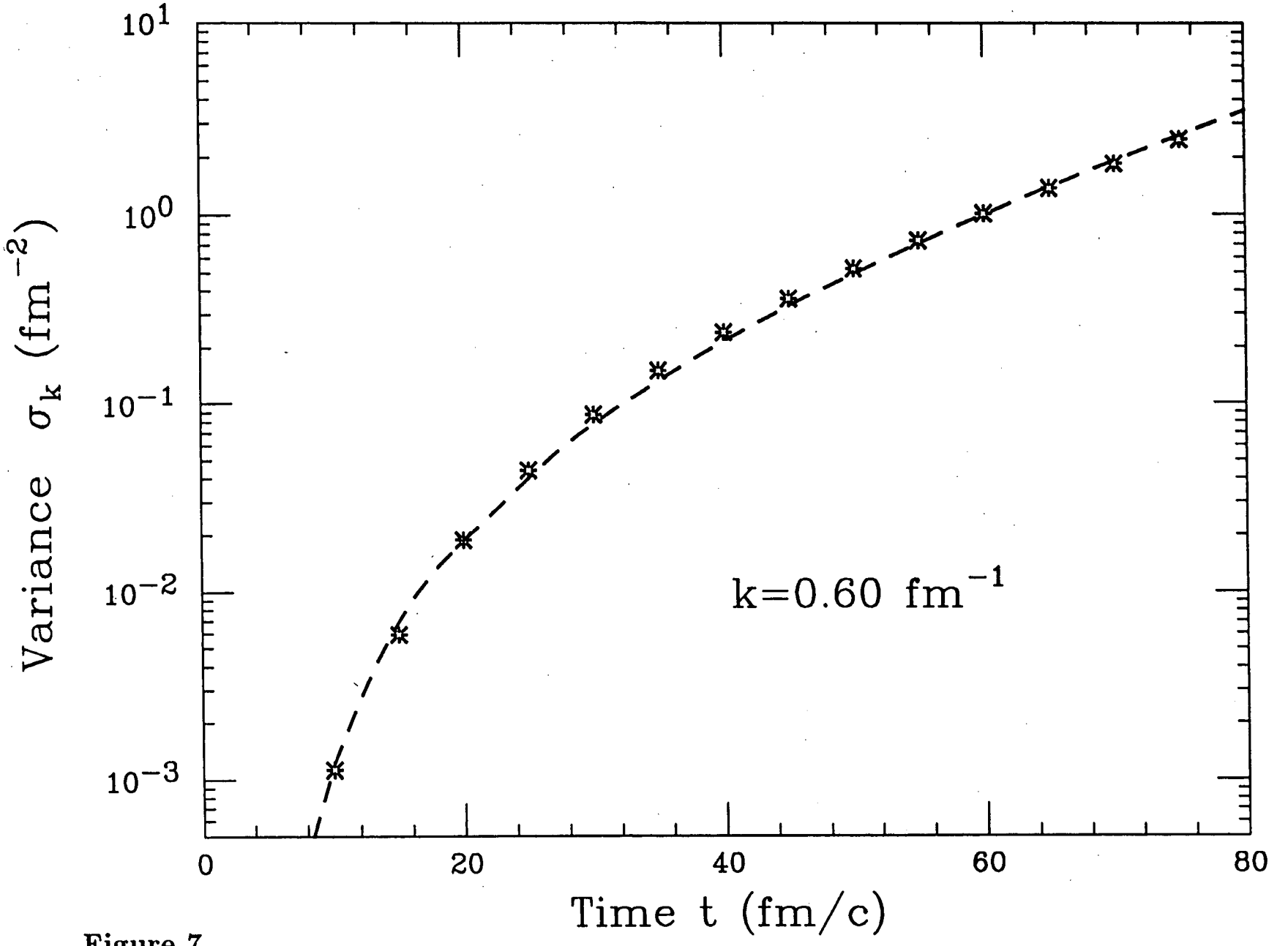
10^1
10^0
10^{-1}
10^{-2}
10^{-3}
Variance σ_k (fm^{-2})
k=0.60 fm^{-1}
0
20
40
60
80
Time t (fm/c)

Figure 7

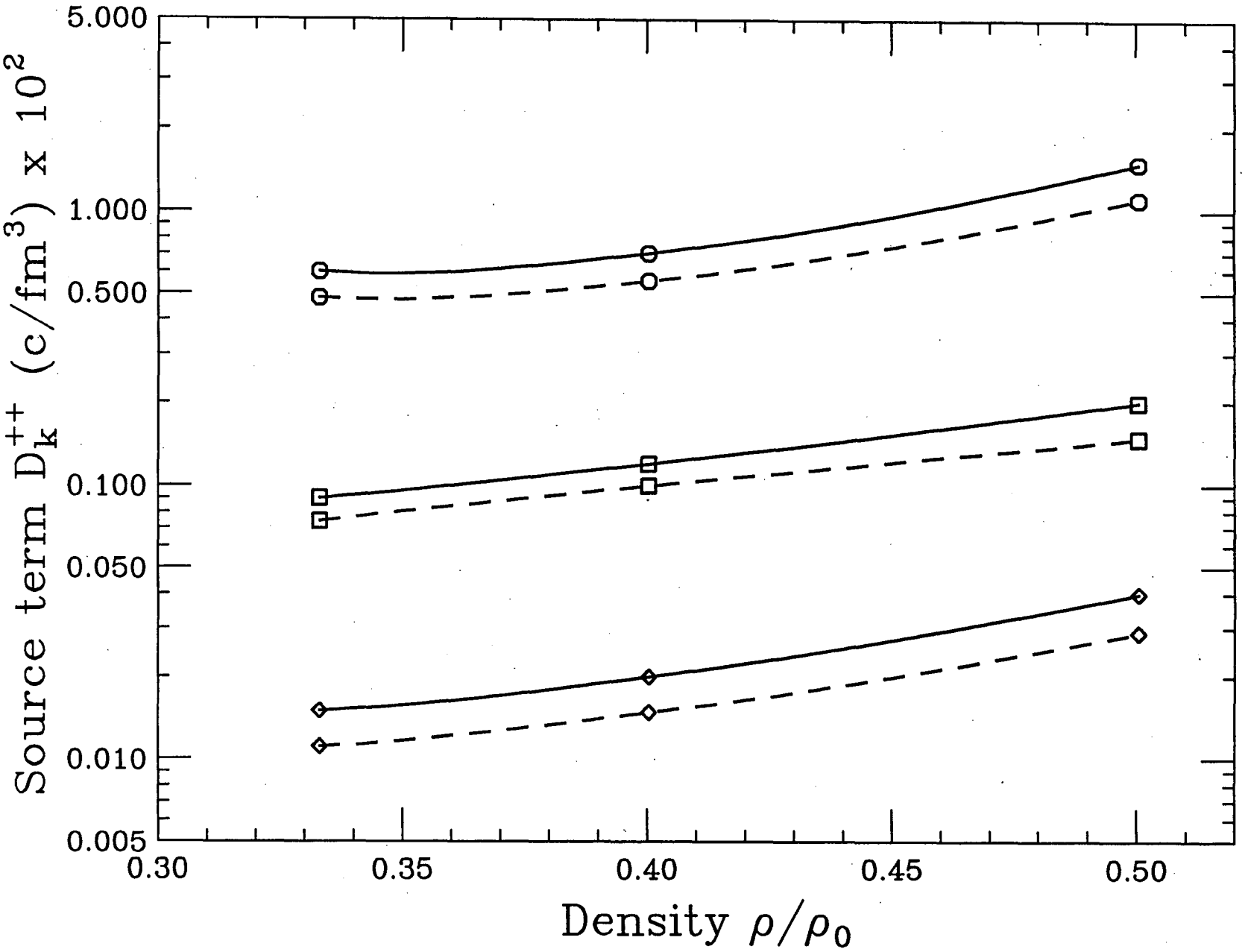
5.000
1.000
0.500
0.100
0.050
0.010
0.005
0.30
0.35
0.40
0.45
0.50
Source term D_k^{++} (c/fm^3) x 10^2
Density ρ/ρ_0

Figure 8

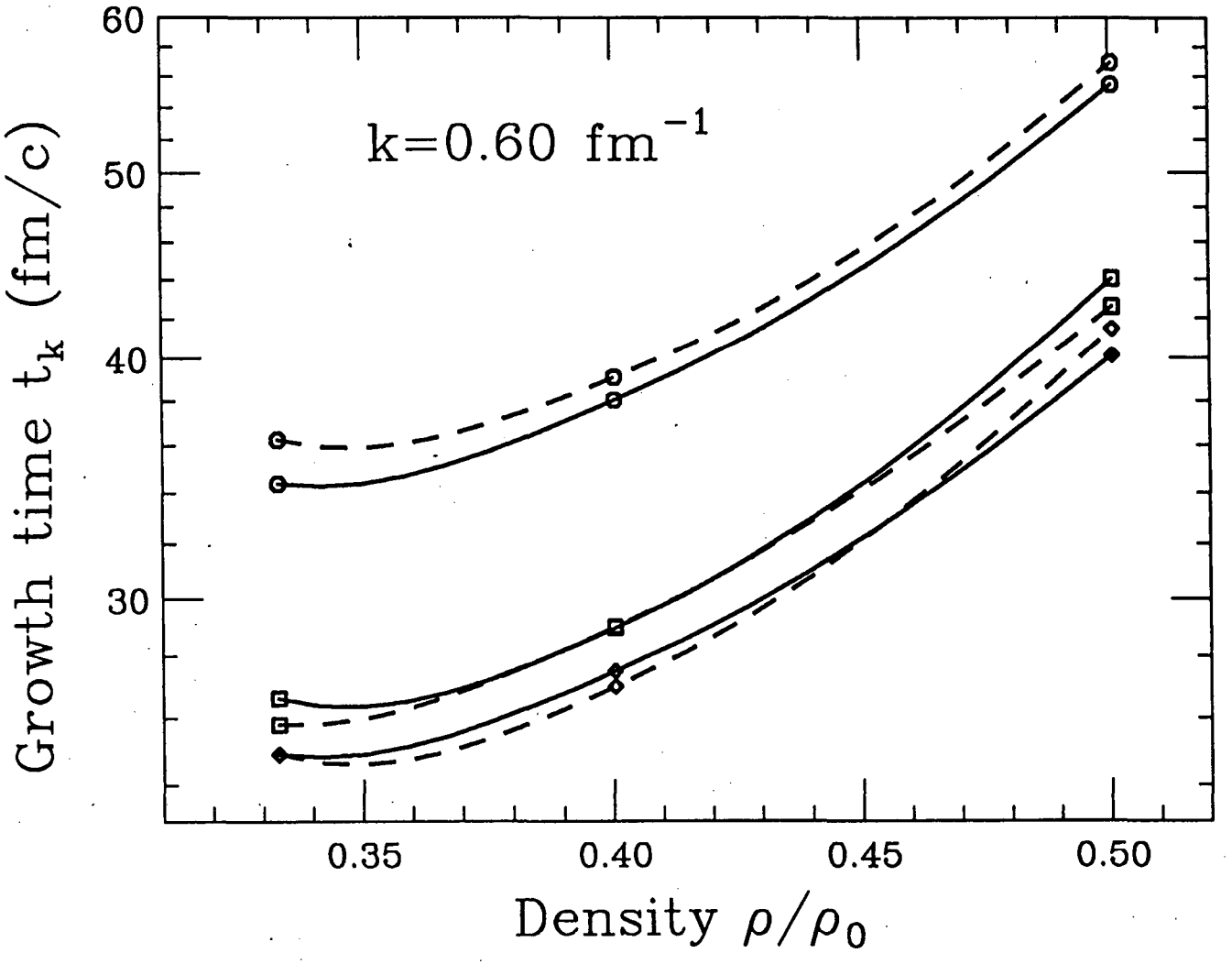
k=0.60 fm^{-1}
Growth time t_k (fm/c)
Density ρ/ρ_0
60
50
40
30
0.35
0.40
0.45
0.50

Figure 9

LAWRENCE BERKELEY LABORATORY
UNIVERSITY OF CALIFORNIA
TECHNICAL INFORMATION DEPARTMENT
BERKELEY, CALIFORNIA 94720